Journal of Hazardous Materials 434 (2022) 128900

Contents lists available at ScienceDirect

Journal of Hazardous Materials

journal homepage: www.elsevier.com/locate/jhazmat

# A polyesterase from the Antarctic bacterium *Moraxella* sp. degrades highly crystalline synthetic polymers

Efstratios Nikolaivits [a], George Taxeidis [a], Christina Gkountela [b], Stamatina Vouyiouka [b], Veselin Maslak [c], Jasmina Nikodinovic-Runic [d], Evangelos Topakas [a,*]

[a] *Industrial Biotechnology & Biocatalysis Group, Biotechnology Laboratory, School of Chemical Engineering, National Technical University of Athens, Athens, Greece*
[b] *Laboratory of Polymer Technology, School of Chemical Engineering, National Technical University of Athens, Athens, Greece*
[c] *University of Belgrade, Faculty of Chemistry, Belgrade, Serbia*
[d] *Eco-Biotechnology & Drug Development Group, Laboratory for Microbial Molecular Genetics and Ecology, Institute of Molecular Genetics and Genetic Engineering, University of Belgrade, Belgrade, Serbia*

## HIGHLIGHTS

- *Moraxella* sp. esterase (MoPE) was found capable of degrading a broad range of synthetic polymers.
- Plastics were ranked based on glass transition temperature, crystallinity and molecular weight.
- MoPE was capable of hydrolyzing high crystallinity PBS while PCL suffered the highest mass loss.
- MoPE mode of action was elucidated by using PET model substrates.
- Terephthalic acid was released from PET by the synergistic action of MoPE with a feruloyl esterase.

## GRAPHICAL ABSTRACT

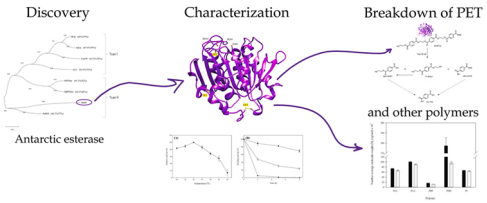


## ARTICLE INFO

*Keywords:*
Plastics degradation
Poly(ethylene terephthalate)
Polycaprolactone
Enzyme
Polyesters

## ABSTRACT

The uncontrolled release of plastics in the environment has rendered them ubiquitous around the planet, threatening the wildlife and human health. Biodegradation and valorization of plastics has emerged as an eco-friendly alternative to conventional management techniques. Discovery of novel polymer-degrading enzymes with diversified properties is hence an important task in order to explore different operational conditions for plastic-waste upcycling. In the present study, a barely studied psychrophilic enzyme (MoPE) from the Antractic bacterium *Moraxella* sp. was heterologously expressed, characterized and its potential in polymer degradation was further investigated. Based on its amino acid composition and structure, MoPE resembled PET-degrading enzymes, sharing features from both mesophilic and thermophilic homologues. MoPE hydrolyzes non-biodegradable plastics, such as polyethylene terephthalate and polyurethane, as well as biodegradable

*Abbreviations:* MHET1, 1-(2-hydroxyethyl)− 4-methylterephthalate; M2HET2.5, 1,4-Benzenedicarboxylic acid, 1,4-bis[2-[[4-(methoxycarbonyl)benzoyl]oxy] ethyl] ester; BHET, Bis(2-hydroxyethyl) terephthalate; DSC, Differential scanning calorimetry; M2HET1.5, Ethylene glycol bis(methyl terephthalate); GPC, Gel permeation chromatography; MHET, Mono-(2-hydroxyethyl) terephthalate; MHET2, Monomethyl bis(2-hydroxyethyl terephthalate); MTPA, Monomethyl terephthalate; MHET3, Monomethyl tris(2-hydroxyethyl terephthalate); pNPB, *p*-nitrophenyl butyrate; PBS, Polybutylene succinate; PCL, Polycaprolactone; PDI, Polydispersity Index; PET, Poly(ethylene terephthalate); PHA, Polyhydroxy alkanoates; PHB, Polyhydroxy butyrate; PLA, Polylactic acid; PU, Polyurethane; TPA, Terephthalic acid; TGA, Thermogravimetric analysis.

* Corresponding author.
*E-mail address:* vtopakas@chemeng.ntua.gr (E. Topakas).

https://doi.org/10.1016/j.jhazmat.2022.128900
Received 28 January 2022; Received in revised form 24 March 2022; Accepted 9 April 2022
Available online 13 April 2022

synthetic polyesters, such as polycaprolactone, polyhydroxy butyrate, polybutylene succinate and polylactic acid. The mass fraction crystallinity of the aliphatic polymers tested ranged from 11% to 64% highlighting the potential of the enzyme to hydrolyze highly crystalline plastics. MoPE was able to degrade different types of amorphous and semi-crystalline PET, releasing water-soluble monomers and showed synergy with a feruloyl esterase of the tannase family for the release of terephthalic acid. Based on the above, MoPE was characterized as a versatile psychrophilic polyesterase demonstrating a broad-range plastics degradation potential.

## 1. Introduction

Since the beginning of the industrial production of plastic resins in the 1950 s, these materials have found applications in every aspect of the human life. Owing to their low manufacturing cost, remarkable properties and versatility, plastics have replaced other materials and plastic components can now be found in almost all items, from electronic devices to buildings and spaceships. The ubiquity of plastics in combination with their inherent resistance to degradation, along with the inefficiency of the current waste management techniques, have led to the accumulation of plastic waste. Especially, today's mentality of single-use products (mostly packaging) has led to the increase of plastic in municipal waste to over 10% (Jambeck et al., 2015). Unfortunately, plastic waste can be also found in large quantities in the oceans, sea floor, Arctic sea ice and even the most remote regions of the planet, such as mount Everest (Jambeck et al., 2015; Napper et al., 2020; Peeken et al., 2018).

Even though biodegradable plastics had emerged as a solution to the plastic pollution problem, their degradation rates in the environment are still much slower than their release rates and especially in marine environments, where these degradation rates are comparable to non-biodegradable plastics (Chamas et al., 2020). Hence, uncontrolled use and release of these plastics would have similar effects to the already used ones (Narancic and O'Connor, 2019).

A new concept for plastic waste management has been introduced in the recent years in the frame of chemical/feedstock recycling; that of plastic upcycling via enzymatic depolymerization to yield monomers/oligomers that are valorized using chemical technologies or biotechnology (fermentation) for the production of new polymers or other value-added products (Blank et al., 2020; Nikolaivits et al., 2021). The depolymerization step is really important in order to achieve high purity of the resulting monomers. A combination of polymer pretreatment and the use of enzymatic catalysts can make such a process feasible for large-scale, as analyzed for the production of terephthalic acid (TPA) from waste poly(ethylene terephthalate) (PET) (Singh et al., 2021). The same rational can be applied to other plastics, including biodegradables, for the recovery of their monomers and their subsequent fermentations in order to produce bioplastics, natural surfactants or other value-added products (Nikolaivits et al., 2021).

Esterolytic microbial enzymes, belonging to different families (cutinases, lipases, esterases), have been proven capable of degrading polyesters such as PET, polylactic acid (PLA), polycaprolactone (PCL) and polyhydroxyalkanoates (PHAs) with varying yields and rates (Nikolaivits et al., 2021; Urbanek et al., 2020). These enzymes can also be designated as depolymerases, owing to their ability to degrade insoluble polymeric materials. The need to discover new efficient depolymerases is urgent at this point in order to develop sustainable plastic waste management processes.

Even though it has been a long-standing belief that depolymerization reactions are enhance above the polymer glass transition temperature, this seems to be disputed by recent studies (Thomsen et al., 2022). However, this belief focused most research on thermophilic polymer-degrading enzymes, neglecting other candidates. For instance, marine biodiversity is an intriguing place to look for biocatalysts that can degrade xenobiotics, due to the fact that pollutants and wastes tend to end up in these environments (Nikolaivits et al., 2017). Additionally, microorganisms isolated from cold marine habitats, including Antarctica, have shown potential in degradation of plastics at low temperatures (Urbanek et al., 2018, 2021).

The goal of the present work was to discover a novel enzyme with potential polyesterase activity and study its ability to degrade a broad range of synthetic materials considered as non-biodegradable, such as PET and polyurethane (PU), as well as a range of biodegradable plastics. Towards this end, a sequence from the Antarctic bacterium *Moraxella* sp. was selected, cloned and expressed in *Escherichia coli*. The resulting recombinant enzyme (MoPE) was biochemically characterized and its polyesterase activity was verified on various polymeric materials with increased crystallinity. The commercial polymeric materials tested were characterized and ranked based on glass transition, mass crystallinity values and number-average molecular weight. MoPE was active on PET model substrates (degree of polymerization 1–3) and its mode of action was elucidated. The enzyme was tested for the degradation of different types of amorphous and semi-crystalline PET materials, while the synergistic interaction with a feruloyl esterase of the tannase family was highlighted for the release of TPA.

## 2. Materials and methods

### 2.1. Structure prediction and protein sequence analysis

The AlphaFold generated structure of MoPE was downloaded from UniProtKB (identifier AF-P19833-F1) and visualized by UCSF Chimera v1.15. The N-terminal sequence (aa 29–54), was excluded from the visualized model, due to the lack of secondary structure information and because it does not align with structures of other polyesterase structures. Structural alignment of protein sequences was performed by UCSF Chimera v1.15 (Pettersen et al., 2004) and visualized by ESPript 3.0 (Robert and Gouet, 2014). Construction of the phylogenetic tree was done by MEGA 7.0 using the structural alignment (Kumar et al., 2016).

### 2.2. Cloning and expression of MoPE gene and purification of recombinant enzyme

Gene coding for the putative polyesterase from *Moraxella* sp. (UniProtKB ID: P19833 excluding the native signal peptide) was synthesized, codon optimized for expression in *E. coli* and cloned in expression vector pET22b(+) by GenScript Biotech (the Netherlands). MoPE expression in *E. coli* BL21 was induced by 0.2 mM isopropyl $\beta$-D-1-thiogalactopyranoside (IPTG) at 16 °C for 20 h, based on the method described previously (Dimarogona et al., 2015). After that time, *E. coli* cells were harvested by centrifugation at 4000g for 15 min at 4 °C and resuspended in 50 mM Tris-HCl pH 8, 300 mM NaCl buffer. Cell suspension was disrupted by sonication during four 1-min cycles (8 s pulses and 5 s pause) at 40% amplitude using a 20 kHz high intensity (400 W) ultrasonic processor (VC 400, Sonic & Materials, Newtown, CT, USA). Cell debris was removed by centrifugation at 20,000g, 30 min, 4 °C twice and loaded onto an immobilized metal-ion ($Co^{2+}$) affinity chromatography (IMAC), as described previously in (Nikolaivits et al., 2016). The purity of isolated enzymes was checked on SDS-PAGE electrophoresis (12.5% polyacrylamide) and protein concentration was determined by measuring the absorbance at 280 nm, based on the molar extinction coefficient (47245 $M^{-1}$ $cm^{-1}$) calculated by ProtParam tool from ExPASy (Gasteiger et al., 2005).

### 2.3. Biochemical characterization of recombinant MoPE

A standard activity assay for MoPE was performed using *p*-nitrophenyl butyrate (*p*NPB) as substrate at 1 mM concentration in 0.1 M phosphate-citrate buffer pH 6. Reactions were initiated by adding 20 μL of enzyme preparation in 230 μL of substrate and the release of *p*-nitrophenol was recorded by measuring the absorbance at 410 nm in a SpectraMax-250 microplate reader (Molecular Devices, Sunnyvale, CA, USA) equipped with SoftMaxPro software (version 1.1, Molecular Devices, Sunnyvale, CA, USA) set at 30 °C.

The effect of temperature and pH on the activity of MoPE was tested by performing the standard assay by either altering the temperature or the pH in the range of 20–50 °C and pH 3–8. Buffer systems used were phosphate-citrate pH 3–6, sodium phosphate pH 6–8 and Tris-HCl pH 8–9 at a concentration of 0.1 M.

The effect of temperature on the stability of MoPE was studied by incubating the enzyme in 20 mM Tris-HCl pH 8 buffer at temperatures in the range of 30–50 °C for up to 8 h and measuring residual activity by standard assay. The effect of pH on the stability of MoPE was studied by incubating the enzyme at 4 °C in 0.2 M of different buffer systems in the range of pH 5–10 for 24 h and then measuring residual activity by standard assay. Buffer systems used were citrate-phospate pH 5–6, sodium phosphate pH 6–8, Tris-HCl pH 8–9 and Glycine-NaOH pH 9–10.

The kinetic characteristics of MoPE were studied on four different *p*-nitrophenyl fatty-acid esters with varying chain length at standard assay conditions. Esters used were: *p*NP-acetate ($C_2$), *p*NPB ($C_4$), *p*NP-octanoate ($C_8$) and *p*NP-decanoate ($C_{10}$). Kinetic constants were estimated using a non-linear regression model in GraphPad Prism 5 from GraphPad Software, Inc. (USA).

### 2.4. Commercial polymeric materials and their mechanical treatment

Commercial polymeric grades were used: PET (PAPET clear, Lotte Chemical, UK), PLA (4043D, NatureWorks, USA), PHB (Biomer P226, Biomer, Germany), PCL (CAPA 6500, Ravago Chemicals, Belgium), aged PBS (initial grade NaturePlast PBE003, NaturePlast, France) and PU (LPR7560, Coim, Laripur). All the resins were in the form of pellets and were cryomilled in a PULVERISETTE 14 (FRITSCH Corp., Idar-Oberstein, Germany). A number of pellets was first immersed in liquid nitrogen and then inserted into the mill at 17000 rpm with additional liquid nitrogen to prevent sintering. The particle size of the resulting powders was < 500 μm. Prior to any characterization, the polymer powders were dried under vacuum (300 mbar); PET was dried at 140 °C for 8 h, PLA and polybutylene succinate (PBS) at 80 °C for 5 h, PHB at 60 °C for 2 h, PCL at 40 °C for 24 h and PU at 90 °C for 3 h.

### 2.5. Material characterizations

#### 2.5.1. Solution viscometry

Solution viscometry was used to define PET powder's number-average molecular weight ($\overline{M_n}$). All the other polymer powders' average molecular weights were defined via GPC.

PET materials were dissolved at room temperature in 1,1,1,3,3,3-hexafluro-2-propanol (HFIP 99%, Fluorochem, UK), at a concentration of 0.2 g/100 mL, and filtered prior measurement using a disposable membrane. Intrinsic viscosity ([η], dL $g^{-1}$) values were determined using a Cannon-Ubbelohde Semi-Micro viscometer (Size 75, K=0.008117 $mm^2$ $s^{-2}$, Cannon Instrument Company, US) and Eq. (1):

$$[n] = \frac{1}{C}\sqrt{2\left(\frac{t}{t_0} - \ln\frac{t}{t_0} - 1\right)} \quad (1)$$

where t is the flow time of solution, $t_0$ is the flow time of pure solvent and C the concentration of the solution.

Measurements were performed in duplicates, at 30 ± 0.1 °C. The intrinsic viscosity was converted to number-average molecular weight via Eq. (2) (Filgueiras et al., 2011):

$$[n] = 4.86 \cdot 10^{-4} \overline{M_n}^{0.72} \quad (2)$$

#### 2.5.2. Thermal properties

Differential scanning calorimetry (DSC) measurements were performed in a Mettler DSC 1 STARe System through heating – cooling – heating cycles (PET: 30–300 °C, PLA: 30–200 °C, PHB and PU: 25–200 °C, PCL: 25–90 °C, PBS: 25–150 °C), under $N_2$ flow (20 mL $min^{-1}$), with heating and cooling rates 10 °C $min^{-1}$. The melting points derived from the first and second heating cycle are represented as $T_{m1}$ and $T_{m2}$, and the relevant mass fraction crystallinity ($x_c$, %) was computed according to Eq. (3). The crystallization point ($T_c$) as well as the crystallization enthalpy ($\Delta H_c$, J $g^{-1}$) were obtained from the DSC cooling cycle.

$$x_C = 100 \cdot \frac{\Delta H_f}{\Delta H_0} \quad (3)$$

where $\Delta H_f$ is the heat of fusion (J $g^{-1}$), $\Delta H_0$ is the heat of fusion of 100% crystalline polymer (J $g^{-1}$) equal to 140 J $g^{-1}$ for PET (Wu et al., 2020), 93.1 J $g^{-1}$ for PLA (Porfyris et al., 2018), 146 J $g^{-1}$ for PHB (Chan et al., 2004), 139 J $g^{-1}$ for PCL (Patrício and Bártolo, 2013) and 110.5 J $g^{-1}$ for PBS (Gkountela et al., 2021).

Thermogravimetric analysis (TGA) was conducted in a Mettler TGA/DSC 1 thermobalance from 30° to 550°C for PET, PBS, PU and PCL resins and 430 °C for PLA and PHB at a heating rate 10 °C $min^{-1}$ under $N_2$ flow (10 mL $min^{-1}$). The onset decomposition temperature was defined as the temperature at 5% weight loss ($T_{d,5\%}$), the degradation temperature ($T_d$) was determined at the maximum rate of weight loss, and the char yield as the % residue at 550 °C for PET, PBS, PU and PCL and 430 °C for PLA and PHB.

### 2.6. Hydrolysis of PET model substrates

MoPE's potential for PET degradation was assessed through reactions with PET model substrates. Reactions were performed in 0.1 M phosphate buffer pH 7, at a substrate concentration of 1 mg $mL^{-1}$ for 24 h at 30 °C under shaking (1200 rpm) in an Eppendorf Thermomixer Comfort (Eppendorf, Germany). The substrates used were monomethyl terephthalate (MTPA), bis(2-hydroxyethyl) terephthalate (BHET), 1-(2-hydroxyethyl)− 4-methylterephthalate (M(HET)1), monomethyl bis(2-hydroxyethyl terephthalate) (M(HET)2) and monomethyl tris(2-hydroxyethyl terephthalate) (M(HET)3), respectively. Moreover, ethylene glycol bis(methyl terephthalate) (M2(HET)1,5) and 1,4-benzenedicarboxylic acid, 1,4-bis[2-[[4-(methoxycarbonyl)benzoyl]oxy] ethyl] ester (M2(HET)2,5) which constitute of 1.5 and 2.5 dimethylated PET monomers were also used (Djapovic et al., 2021).

Supernatants of these reactions were analyzed on a SHIMADZU LC-20 CE HPLC equipped with a SIL-20A autosampler. The column used was a C-18 reverse-phase NUCLEOSIL®100–5 (Macherey-Nagel,Germany) and the mobile phase was 20% (v/v) acetonitrile, 20% (v/v) 10 mM sulfuric acid in 60% (v/v) ultrapure water at a flow rate of 0.8 mL $min^{-1}$. Detection of TPA and its derivatives took place with a photodiode array detector Varian ProStar at 241 nm. Prior to analysis 0.1% (v/v) of 6 M HCl was added in each reaction and centrifuged at 5000 x g, 10 °C. Supernatants were filtered through 0.2 μm syringe filters and analyzed. Quantification of TPA, mono-(2-hydroxyethyl) terephthalate (MHET) and BHET was performed by constructing calibration curves with standard concentrations in the range of 0.01–1 mM. MHET was prepared by BHET following the method of Furukawa et al. Furukawa et al. (2018).

### 2.7. Hydrolysis of different synthetic polymeric materials

MoPE's ability to degrade polyesters was tested in reactions containing 10 mg $mL^{-1}$ of polymeric powder (particle diameter < 500 μm)

in 0.1 M phosphate buffer pH 7 incubated at 30 °C under agitation (1200 rpm) in an Eppendorf Thermomixer Comfort (Eppendorf, Germany) for three days. Reactions were initiated by the addition of 50 μg MoPE while another 25 μg of enzyme were supplemented after 24 and 48 h. At the end of the reactions, the residual material was isolated by centrifugation, washed with ultrapure water twice, freeze-dried and its weight was measured.

For the determination of the molecular weights of enzyme-treated materials, gel permeation chromatography (GPC) was carried out with the use of an Agilent 1260 Infinity II instrument (Agilent Technologies, Germany), equipped with a guard column (PLgel 5 μm) and two PLgel MIXED-D 5 μm columns (300 ×7.5 mm). Elution was carried out with tetrahydrofuran (THF >=99.9% purity, Macron Fine Chemicals, Poland) or chloroform (>= 99.8% purity, Fisher Chemical, U.K.) at a flow rate of 1 mL $min^{-1}$. THF was used for the molecular weight determination of PU, PCL and PLA samples, whereas PBS and PHB samples were analyzed using chloroform. The analysis was performed using an Agilent 1260 Infinity II refractive index detector (RID) (G7162A). The calibration of the instrument was carried out with polystyrene standards of molecular weight from 162 to 500.000 g/mol (EasiVial PS-M 2 mL, Great Britain).

In the case of PET degradation, the reaction supernatants were analyzed with HPLC as described above for the quantification of water-soluble hydrolysis products.

### 2.8. Synergy study of MoPE with FoFaeC for PET degradation

The synergistic relationship of MoPE with a feruloyl esterase from *Fusarium oxysporum*, FoFaeC (Moukouli et al., 2008), was tested on different PET materials in reactions performed as described above, but with the addition FoFaeC at 25 μg at time zero, while another 12 μg were added once per day for the next two days. In this way, the mass ratio of MoPE /FoFaeC was kept constant and equal to 2:1. In the case of PET degradation by FoFaeC alone, 25 μg of enzyme were added at time zero, while half amount was added once per day for the next two days, as mentioned above.

## 3. Results and discussion

### 3.1. Comparison of MoPE sequence and structure to known polyesterases

The selected amino acid sequence (Feller et al., 1990), namely MoPE, originates from the bacterium *Moraxella* sp TA144, isolated from Antarctic sea water and has been designated as a triacylglycerol lipase by UNIPROT (entry P19833). According to BLASTp, this enzyme shares the highest similarity (> 67%) with α/β hydrolases, lipases and hypothetical

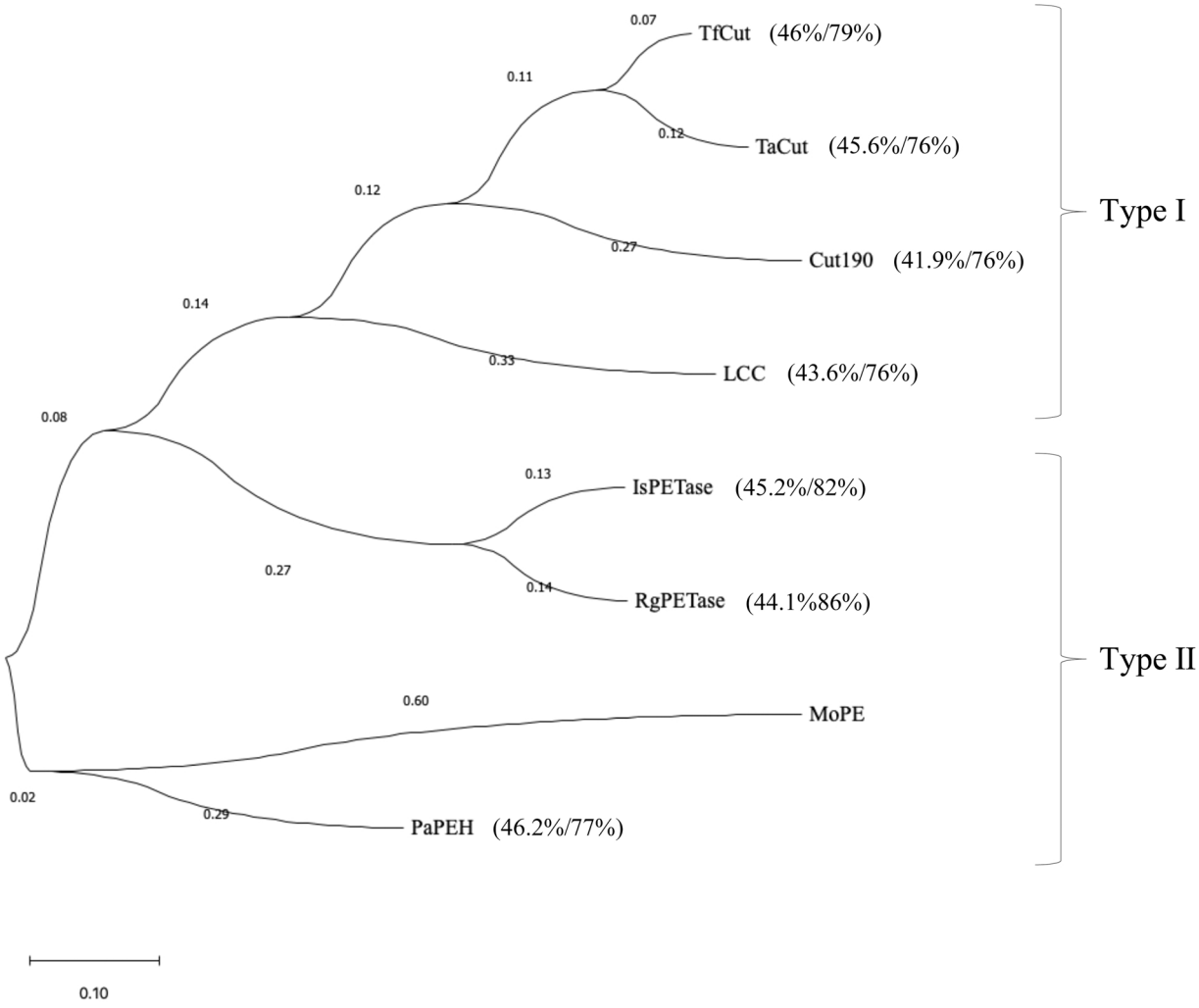


**Fig. 1.** Phylogenetic tree of selected Type I and Type II PET-hydrolases constructed by the Maximum-Likelihood Method and visualized by MEGA 7. Next to the name of each enzyme, the percentage identity to MoPE for percentage sequence coverage is presented in parenthesis. Selected PET-hydrolases: *Thermobifida fusca* cutinase 2 (TfCut), *Thermobifida alba* cutinase Est199 (TaCut), *Saccharomonospora viridis* Cut190 (Cut190), Leaf-branch Compost cutinase (LCC), *Ideonella sakaiensis* PETase (IsPETase), *Rhizobacter gummiphilus* PETase (RgPETase), *Pseudomonas aestusnigri* Polyester Hydrolase (PaPEH).

proteins from various *Psychrobacter* species. Concerning characterized enzymes, MoPE shows the highest percentage identity (42–46%) with confirmed PET-hydrolases (Fig. 1) and is more closely related to other Proteobacterial PETases belonging to Type II class, compared to thermophilic Actinobacterial cutinases that are categorized as Type I.

Structure-based alignment of MoPE with other polyesterases (Fig. 2) confirms this fact, as MoPE contains a second disulfide bridge (Cys231-Cys266), characteristic of Type II enzymes, in addition to the first disulfide bond (Cys299-Cys318) that is present in both Type I and Type II enzymes. MoPE's model, however, suggests that this enzyme may also possess a third disulfide bond (Cys60-Cys109) connecting its N-terminal loop with a $3_{10}$ helix (η2) between beta-sheets β2 and β3. This $3_{10}$ helix is predicted only on MoPE, while all the other structures present a loop at the same point (Fig. 3). It is also worth mentioning that the N-terminal sequence (aa 55–66) of MoPE (where C60 is located) varies greatly compared to the rest of PET-degrading enzymes studied, on which this region is conserved (for instance aa 30–36 for IsPETase and 37–43 for LCC). The presence of an additional disulfide bridge has also been suggested by (Blázquez-Sánchez et al., 2022) but it was not thoroughly proven experimentally.

The conserved Phe in thermophilic cutinases, is also Phe265 in MoPE, but in other Type II enzymes this residue is a conserved Ser. On the other hand, the conserved Trp in all shown polyesterases (for instance Trp185 in IsPETase) is Tyr214 in MoPE. This "wobbling" Trp has shown to be an important feature of PET-degrading polyesterases in combination with a Ser and an Ile (Ser214 and Ile218 in IsPETase). The presence of all three residues enhances the PETase activity of most homologous enzymes (Chen et al., 2021). In the case of MoPE Ser is substituted by Tyr242 (His in all other enzymes) and Ile is substituted with Phe246 as in all other enzymes (Fig. S1). These findings give ground for site-directed mutagenesis studies in order to prove this theory and enhance the PET-degrading activity of MoPE.

Comparison of LCC's substrate binding sites (Tournier et al., 2020) to MoPE shows many similar features (Fig. 4). Subsite − 2 (green) in LCC comprises of Tyr95, Phe125, Tyr127, Met166, Trp190 and Ala213, while the respective residues in MoPE are Tyr121, Tyr151, Asp153, Met190, Tyr214 and Ala237. The most striking differences are Tyr151 in MoPE, that is either Phe or Lys in other polyesterases (Lys127 in IsPETase), while Asp153 is Gln in all other polyesterases (Gln119 in IsPETase) except from LCC. Subsite − 1 (yellow) in LCC contains residues Gly94, Thr96, His164, Ser165 (catalytic), Asp210 (catalytic), Val212 and His242 (catalytic), while the respective ones in MoPE are Gly120, Val122, Trp188, Ser189, Asp234, Ile236 and His264. In this subsite, apart from the catalytic residues and Gly119, which is conserved in all polyesterases, the rest of the residues differ. Val122 in MoPE is Thr in all other polyesterases except from PaPEH (there is also Val). Trp188 is conserved in all Type II enzymes, while in all Type I enzymes is His. On the other hand, Ile236 present in MoPE is conserved for all polyesterases except from LCC. Regarding subsite + 1 (blue), LCC and MoPE share two of the three residues Ser and Phe (Ser127 and Phe265 in MoPE), but not the third one which is an Ans in LCC and all other polyesterases, but a Ser in MoPE (Ser268). Ser127 is conserved in all polyesterases, while Phe265 is conserved in the thermophilic cutinases, but the respective residue in TypeII enzymes (and MoPE) is a Ser. These observations suggest that MoPE shows similar features to both psychrophilic PET hydrolases, but also to their thermophilic counterparts.

### 3.2. Biochemical characterization of MoPE

The native sequence of the putative lipase enzyme (UniProtKB ID: P19833) contains a signal peptide (aa 1–28: MFIMIKKSELAKAIIVTGALVFSIPTLA) identified by SignalP v5.0 tool (Almagro Armenteros et al., 2019) and excluded from cloning. The theoretical molecular weight (MW) of the recombinant enzyme was calculated by ExPASY ProtParam tool (Gasteiger et al., 2005) to be 32946 Da. MoPE was recombinantly expressed and purified to homogeneity and its biochemical properties determined. The purified enzyme appeared as a single band in SDS-PAGE gel at ~33 kDa (Fig. S2). Even though this enzyme derives from a cold environment, its optimum activity temperature was detected at 30 °C, while it retained over 80% of its maximum activity at a temperature range of 20–35 °C. Beyond this temperature, the enzyme linearly loses activity up to 45 °C, while at 50 °C MoPE retains 10% of its optimal activity (Fig. 5A). At its optimum activity temperature, the enzyme seems to be fairly stable experiencing less than 20% loses after 5 h (Fig. 5B). On the contrary, at higher temperatures, MoPE seems to be rather thermolabile. At 40 °C its half-life was 2 h, while at 50 °C it loses 90% of its activity after just 2 h (Fig. 5B). When Blázquez-Sánchez et al. Blázquez-Sánchez et al. (2022) studied the optimum PCL-degradation temperature of a truncated MoPE construct (Mors1) they found it was 25 °C, while at 50 the enzyme lost 95% of its activity. Nano differential scanning fluorimetry showed that the enzyme's melting temperature was 52 °C, but 31 °C was the onset temperature for denaturation.

The dependence of the activity on the pH can be seen in Fig. S3. Above pH 8 activity seems to increase dramatically. However, it was impossible to test the activity above pH 9 since the autohydrolysis of the substrate is really high at alkaline pH. In order to study the stability of MoPE in different pH, the enzyme was incubated in different buffer systems of 200 mM ionic strength and its activity compared to the enzyme incubated in 20 mM Tris-HCl pH 8, which was the standard storage buffer. For all buffer systems tested (pH 5–10) the enzyme was more stable compared to the storage buffer. Apparently, the ionic strength of the buffer is more important for enzyme stability than the pH itself, even though at pH 5–6 MoPE seemed to be more stable. Enhancement of stability at higher salt concentrations may be due to the fact that this enzyme derives from a marine source. Furthermore, Blázquez-Sánchez et al. Blázquez-Sánchez et al. (2022) noticed a 20% increase in activity of Mors1 by the addition of 200 mM NaCl in the reaction mixture, as it is typical for psychrophilic enzymes.

Determination of MoPE's kinetic constants on water-soluble fatty acid esters cannot necessarily be correlated with its ability to degrade polymers, but is useful in order to compare it with other polyesterases. *p*-Nitrophenyl esters of 2–10 carbon atom chain-lengths were tested. As shown in Table 1 results, MoPE shows a typical kinetic profile as most microbial cutinases (Nikolaivits et al., 2018). Its $k_{cat}$ for $C_2$ ester is the highest and decreasing by increasing the chain length, reaching a 26-fold drop for $C_{10}$. On the other hand, affinity ($K_M$) reaches a peak for $C_4$ ester, when it's 3- and 4-fold lower for $C_2$ and $C_8$-$C_{10}$, respectively. These lead to much higher catalytic efficiency towards $C_4$ ester followed by $C_2$. The kinetic profile of MoPE seems to be the typical as most microbial cutinases characterized so far (Nikolaivits et al., 2018).

### 3.3. Properties of the target polymeric materials

Six (6) polymers were herein examined starting from commercial grades (Table S1). For PET, PLA and PU the temperature range of the studied enzymatic hydrolysis (30 or 50 °C) was below their $T_g$ values, while for PHB, PBS and PCL, higher segmental mobility in the amorphous regions is expected due to their lower $T_g$s.

Crystallinity plays also a major role in the enzymatic hydrolysis; increased crystallinity limits the movement of polymer chains leading to their decreased availability for enzymatic attack (Mohanan et al., 2020). PBS powder presented the highest mass fraction crystallinity (64%, 2nd heating); it also presented a double-melting behavior with melting endotherms at 109 °C and 115 °C. Such behaviour is typical for aliphatic polyesters like PBS (Wang et al., 2007), and is correlated to the existence of two different crystal populations (e.g. different lamellar thickness) with different thermal stability. On the other hand, PBS initial $\overline{M_n}$ was found to be the lowest (16100 g/mol, PDI=1.7), with single-step degradation at 387 °C, slightly lower than a typical PBS grade of $\overline{M_n}$ 75000 g/mol (ca. 400 °C) (Georgousopoulou et al., 2016). Regarding

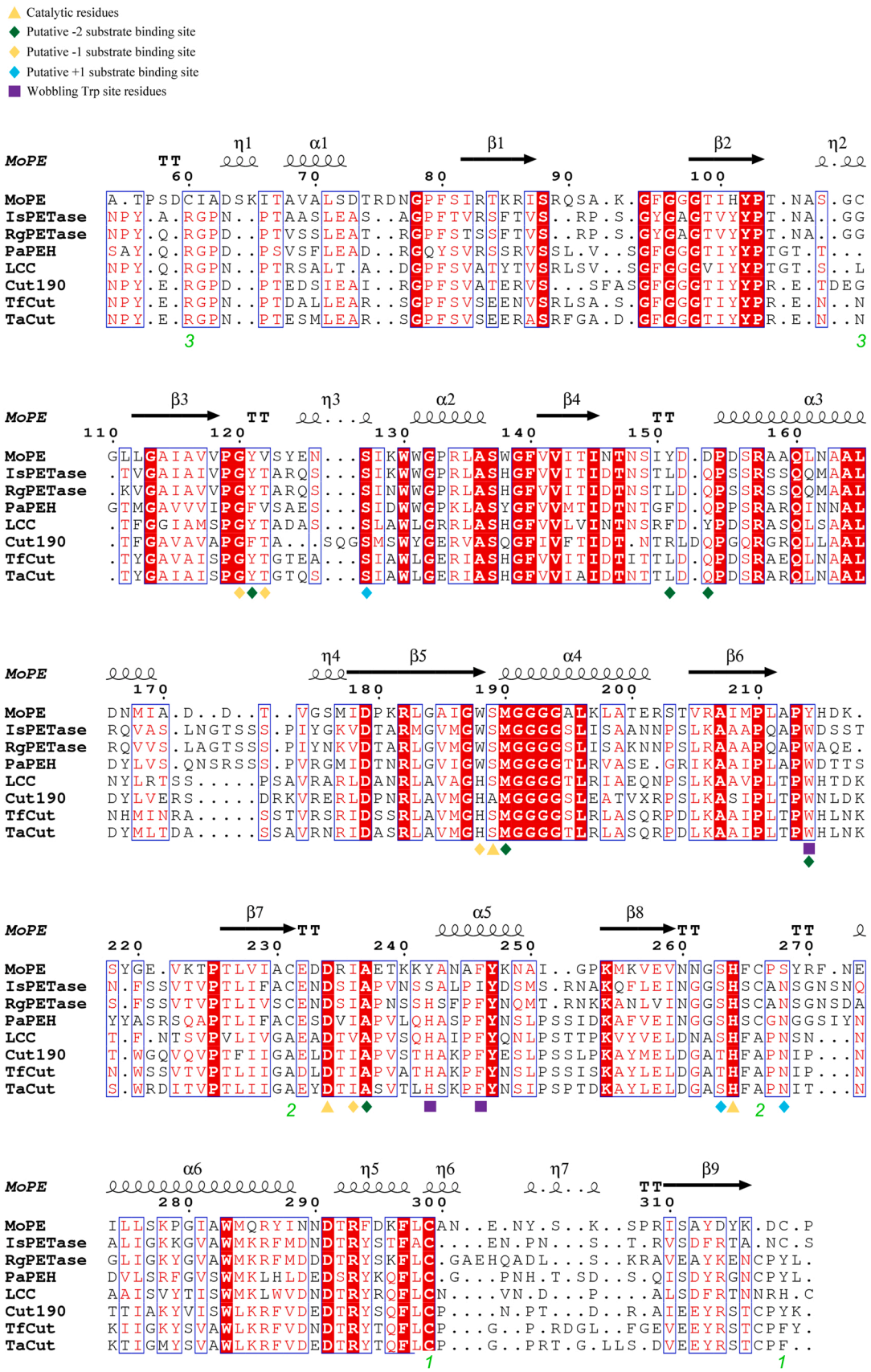


**Fig. 2.** Structure-based multiple sequence alignment of MoPE with characterized polyesterases/PET-degrading enzymes: IsPETase (6EQD), RgPETase (7DTZ), PaPEH (6SCD), LCC (4EB0), Cut190 (5ZRR), TfCut (4CG1) and TaCut (6AID). Disulfide bridges are numbered in neon green, while other important residues are marked as explained on the top of the figure.

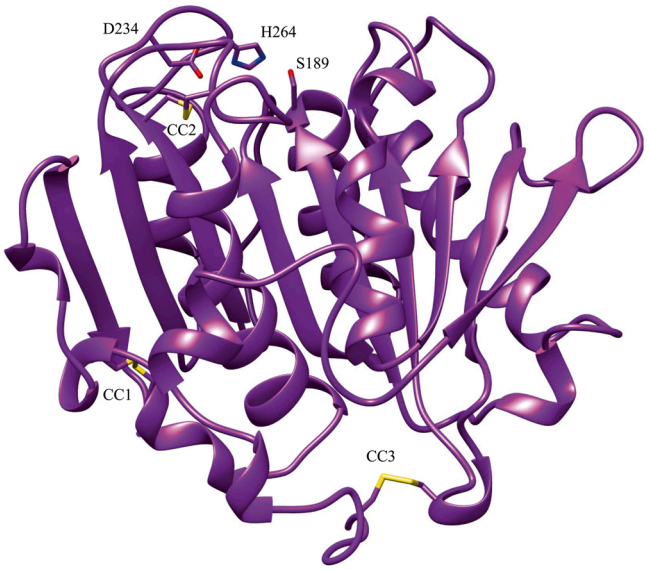


**Fig. 3.** MoPE overall structure, modelled by AlphaFold and visualized in UCSF Chimera v1.15 (excluding residues 29–54), highlighting the three putative disulfide bridges (CC2:Cys231-Cys266, CC1: Cys299-Cys318, CC3: Cys60-Cys109) and the catalytic triad shown as sticks.

PHB powder, crystallinity was also found high (49%) accompanied with a double-melting behaviour. The $\overline{M_n}$ of PHB powder was found 177400 g/mol (PDI=1.2) and the main $T_d$ at 277 °C, indicating increased thermal stability compared to another PHB commercial grade of $\overline{M_n}$ 260000 g/mol (ca. 260 °C) (Mousavioun et al., 2010). PCL crystallinity was found 45% with a single melting point (56 °C) and $\overline{M_n}$ of 73700 g/mol (PDI=1.4). PCL presented also a single-step degradation profile, as expected, with a $T_d$ at 397 °C, being lower than PCL of $\overline{M_n}$ 42500 g/mol (ca 450 °C) (Vogel and Siesler, 2008).

The PET powder presented medium crystallinity of 27%, $T_{m2}$ of 249 °C, $\overline{M_n}$ 35900 g/mol and a single degradation peak at 421 °C, which is slightly lower compared to the reported in literature values of similar molecular-weight PET grades (e.g. $\overline{M_n}$ 34000 g/mol, $T_d$ 451 °C) (Thiyagarajan et al., 2014). PLA powder was also found slightly crystalline, with $x_c$ 11% and $T_{m2}$ 152 °C. PLA $\overline{M_n}$ was equal to 100600 g/mol (PDI=1.5) along with a single-step $T_d$ at 365 °C, indicating decreased thermal stability compared to PLA grades of lower average molecular weight; a commercial PLA grade of $\overline{M_n}$ 84100 g/mol is reported to present a $T_d$ of 384 °C (Xiang et al., 2020). On the other hand, the polyether PU powder was found amorphous ($T_g$ 150 °C) with $\overline{M_n}$ of 66500 g/mol (PDI=1.8). The PU powder presented a two-step thermal decomposition (at 343 and 397 °C), attributed to the coexistence of hard and soft segments in the repeating unit; the first step is the degradation of the urethane groups of hard segments and the second the breaking the ether bonds in soft segments (Kasprzyk et al., 2019).

Summarizing the starting materials characteristics, their ranking regarding glass transition, mass crystallinity values and number-average molecular weight is presented in Table 2, and will be correlated below to enzymatic hydrolysis yield.

### 3.4. Degradation of PET oligomers by MoPE

The activity on MoPE was first tested on various oligomeric PET model compounds (Djapovic et al., 2021) in order to see its potential for PET degradation, but also to try and understand its mode of action. As shown in Fig. 6, MoPE was found capable of cleaving mono- and di-substituted terephthalic acid esters. MTPA was easily cleaved by the enzyme yielding TPA. On the other hand, BHET that is a typical substrate for PETases, was almost completely converted to MHET, with a very small amount of that being cleaved to TPA possibly chemically, due to the buffer's pH. Similarly, M(HET)1 was cleaved to MTPA and MHET. This means that the enzyme cannot clearly distinguish between the methyl and ethyl substitutions, even though it showed some preference towards the cleavage of the ethyl group, since MTPA was the most abundant product (Fig. S4A). This probably means that the enzyme has more affinity towards the MTPA moiety than the MHET moiety.

Regarding substrates with two terephthalate units, MoPE seems to more easily cleave the M(HET)2, than the M2(HET)1,5, whose hydrolysis yielded almost 60-fold lower product concentration. Based on the previous observations about monomer hydrolysis, but also based on the detection of residual BHET and the abundance of each product, we conclude that the main pathway of M(HET)2 degradation should be the recognition and cleavage of MTPA, with concomitant release of BHET, which is readily cleaved to MHET. Of course, part of the substrate would also be cleaved to the MHET moiety, due to the enzyme's versatility. In

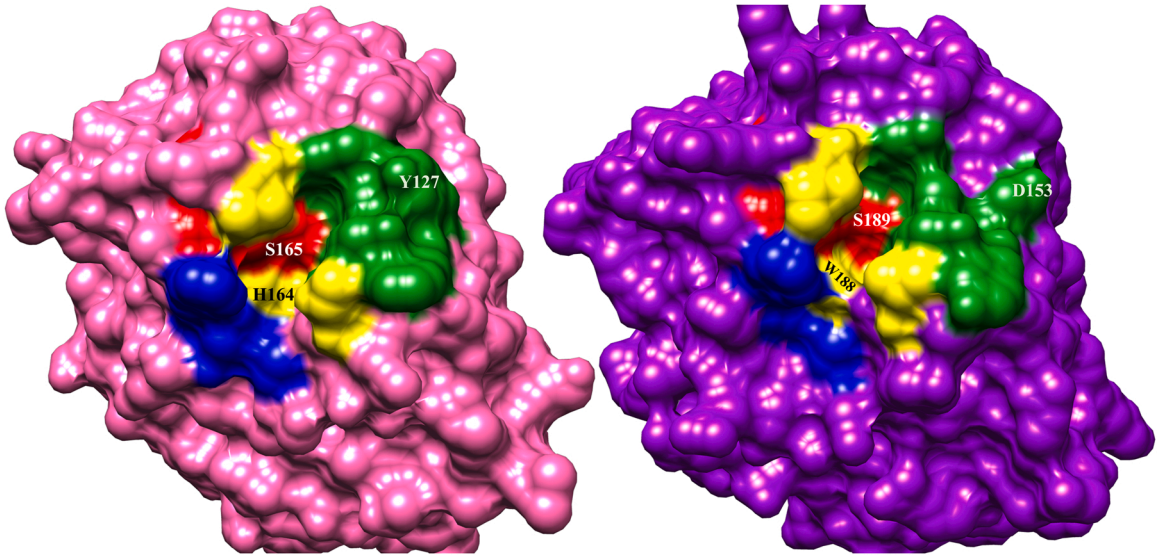


**Fig. 4.** Surface representation of LCC (left-pink) and MoPE (right-purple) structures, highlighting the LCC binding sites with the respective residues in MoPE. Catalytic triad is depicted in red, while subsite − 2 in green, subsite − 1 in yellow and subsite + 1 in blue. The residues that greatly alter the surface of MoPE in comparison to LCC are: Asp153 (Tyr127 in LCC) of subsite − 2 and Trp188 (His164 in LCC) of subsite − 1.

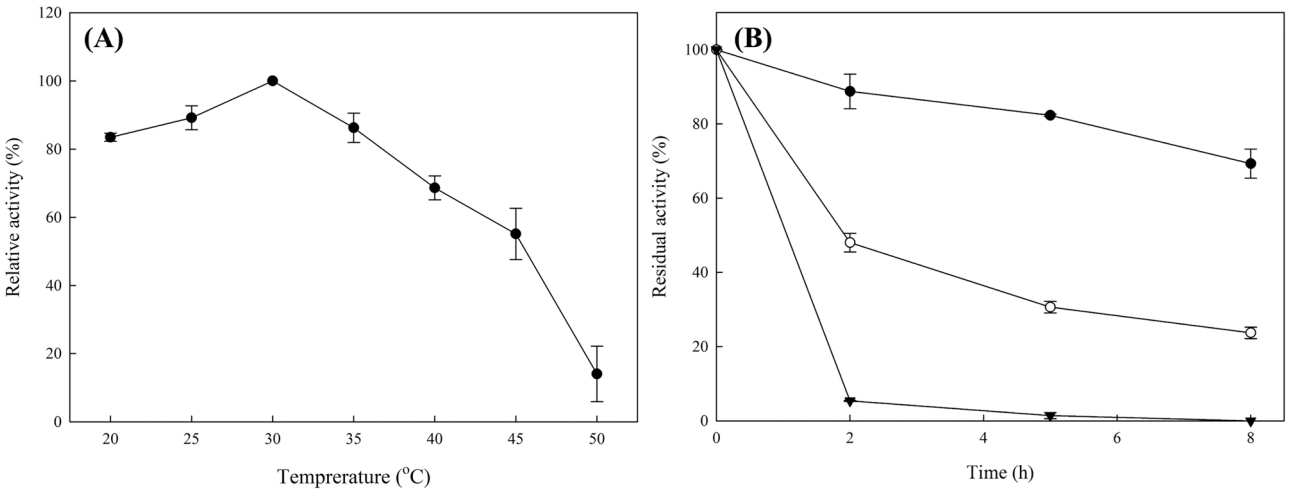


**Fig. 5.** Effect of temperature on the (A) activity and (B) stability of MoPE. For stability experiments, relative activity at 30 (●), 40 (○) and 50 (▼) °C has been calculated based on enzyme incubated in ice.

**Table 1**
Kinetic constants of MoPE on synthetic aliphatic esters.

| Substrate | $k_{cat}$ ($min^{-1}$) | $K_M$ (mM) | $k_{cat}/K_M$ ($min^{-1}$ $mM^{-1}$) |
|---|---|---|---|
| *p*NP-$C_2$ | 69.6 ± 7.7 | 5.4 ± 1.0 | 12.8 ± 2.7 |
| *p*NP-$C_4$ | 29.2 ± 1.3 | 1.7 ± 0.2 | 17.6 ± 2.0 |
| *p*NP-$C_8$ | 5.8 ± 0.7 | 7.2 ± 1.1 | 0.8 ± 0.2 |
| *p*NP-$C_{10}$ | 2.7 ± 0.5 | 7.0 ± 1.8 | 0.4 ± 0.1 |

that case M(HET)1 would also be released and further cleaved to MHET and MTPA (Fig. S4C).

Similarly, but in a much lesser extent, MoPE cleaves M2(HET)1,5 to MTPA and M(HET)1, which is then further hydrolyzed to more MTPA and MHET, like in the case of the respective model compound (Fig. S4B).

Compounds with three terephthalate moieties, M(HET)2,5 and M (HET)3, were hydrolyzed by MoPE in the same degree, which was much lower than for the other substrates. M(HET)2,5 was mostly converted to MTPA and some MHET, when M(HET)3 was hydrolyzed to MHET and MTPA with a small amount of residual BHET (Fig. S4D,E). In all cases small amounts of TPA were also detected, either released chemically or due to the very weak activity of MoPE to MHET and MTPA.

### *3.5. PET degrading ability of MoPE and synergism with FoFaeC for the release of TPA*

MoPE's ability to degrade PET was tested at 30 °C and pH 7 on three different materials to examine two important factors, i.e. the geometry of the substrate and its segmental mobility based on crystallinity values: an amorphous PET film ($x_c$ 0%), an amorphous PET powder ($x_c$ 5%) and the target polymeric material, semi-crystalline PET powder ($x_c$ 41%). As shown in Fig. 7, MoPE could degrade all materials releasing TPA and MHET. The lowest activity was detected on the films compared to both powders, probably due to the much lower reaction surface area.

Interestingly, MoPE could degrade semi-crystalline PET, releasing a total of 1.3 μM water-soluble products. Despite PET's high $T_g$, this high degradation rate can be attributed to water-induced plasticization. Water molecules diffuse between polymer chains and weaken interactions, leading to increased chain mobility and flexibility. As a result, the enzymes accessibility to the PET substrate increases (Kawai et al., 2019). On amorphous PET powder however, the enzyme was more efficient, releasing 3.5 and 6.6-fold higher amount of products compared to semi-crystalline powder and amorphous film, respectively. Higher degradation rates are expected when amorphous polymeric materials are enzymatically hydrolyzed. This is attributed to the effect of crystallinity which limits chains' mobility decreasing their availability for enzymatic attack. For the same reasons, PET bottles and textiles are found less prone to be directly hydrolyzed due to the additional stretch-induced crystallization (Kawai et al., 2019). As for product ratio, TPA was the main degradation product, while MHET accounted for about 40% of total products in case of semicrystalline and amorphous PET powder. When Mors1 was tested on amorphous PET film, it released ca 280 μM of total products after only 24 h. The reaction took place at 25 °C, pH 8 and in the presence of 200 mM NaCl, which is clearly a more advantageous reaction environment for PET degradation (Blázquez-Sánchez et al., 2022). Even though all PET-degrading enzymes have been shown to have activity on amorphous PET materials (Nikolaivits et al., 2021) not many of them have been tested on semi-crystalline PET materials and most of them have been shown to not being able to degrade them. For instance, PaPEH could only hydrolyze amorphous PET film (the product release was not quantified), but it couldn't degrade PET bottle material, which is known to be semi-crystalline (Bollinger et al., 2020). RgPETase has been tested on microcrystalline PET material ($x_c$ 17.1%), releasing around 550 μM of products after 3 days of incubation at 30 °C (Sagong et al., 2021).

As with any natural polymer (eg polysaccharide), the synergistic action of enzymes is needed in order to be broken down into their monomers. As shown in the pioneering work of Yoshida et al. Yoshida et al. (2016), in order for the bacterium *I. sakaiensis* to assimilate PET, it needs and expresses two enzymes IsPETase and IsMHETase; the first one cleaving PET polymer to MHET and the latter cleaving MHET to TPA and EG, which are then used as a carbon source for the bacterium. MHETase belongs to the tannase family and seems to have evolved from feruloyl

**Table 2**
Polymeric materials' ranking based on $T_g$, $x_C$ and $\overline{M_n}$.

| Property | Polymer ranking | | | | | | | | | | | |
|---|---|---|---|---|---|---|---|---|---|---|---|---|
| $T_g$ | PU | > | PET | > | PLA | > | PHB | > | PBS | > | PCL |
| $x_C$ | PBS | > | PHB | > | PCL | > | PET | > | PLA | > | PU |
| $\overline{M_n}$ | PHB | > | PLA | > | PCL | > | PU | > | PET | > | PBS |

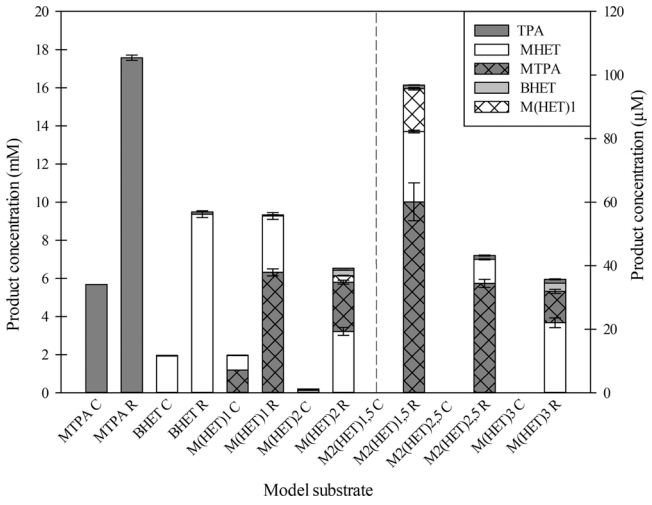


**Fig. 6.** Concentration of water-soluble products detected after the treatment of different PET model compounds with MoPE. Reactions took place at 30 °C for 24 h. Abbreviations of compounds: TPA, terephthalic acid; MTPA, monomethyl terephthalate; BHET, bis(2-hydroxyethyl) terephthalate; MHET, mono-(2-hydroxyethyl) terephthalate; M(HET)1, 1-(2-hydroxyethyl)− 4-methylterephthalate; M(HET)2, monomethyl bis(2-hydroxyethyl terephthalate); M2(HET) 1,5, ethylene glycol bis(methyl terephthalate); M2(HET)2,5, 1,4-benzenedicarboxylic acid, 1,4-bis[2-[[4-(methoxycarbonyl)benzoyl]oxy]ethyl] ester; M (HET)3, monomethyl tris(2-hydroxyethyl terephthalate). Dashed line; left part at mM and right part at μM Y-axis scale.

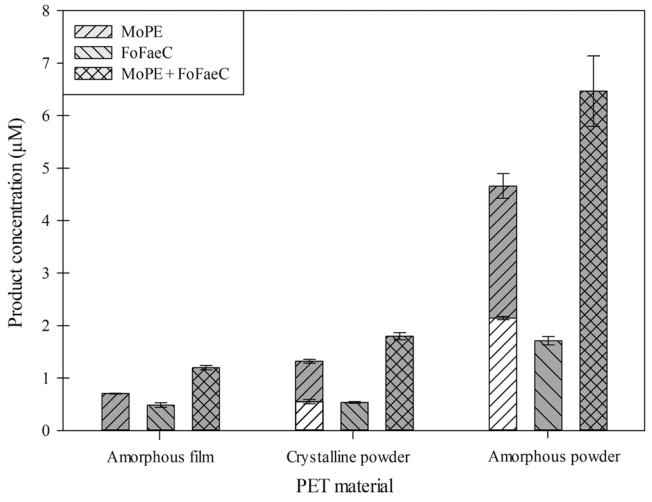


**Fig. 7.** Concentration of released TPA (dark grey bars) and MHET (white bars) after treating different PET materials with MoPE (right diagonal line), feruloyl esterase (FoFaeC) (left diagonal line) and their combined action (crossed lines). The PET materials tested include amorphous PET (0.66 mm thickness), amorphous powder (ca 5% crystallinity) and powder of 35% crystallinity (< 500 μm diameter).

esterases (Knott et al., 2020). For this reason, FoFaeC, a feruloyl esterase belonging to the tannase family (Dimarogona et al., 2020), was employed in the present study in an attempt to complement MoPE at the degradation of different PET materials. The goal was to yield as pure TPA as possible without the presence of MHET.

FoFaeC alone could release small amounts of water-soluble monomers from all tested materials, but lower than MoPE. When the two enzymes were added simultaneously, the degree of synergism (DS) to TPA was 1.5 and 1.4 for amorphous and crystalline powder, respectively, while no such relationship was shown for the films.

### 3.6. MoPE potential to degrade synthetic semicrystalline polymers

Antarctic bacteria have shown great potential in breaking down biodegradable and non-biodegradable polymers (Urbanek et al., 2021; Habib et al., 2020), meaning that they are capable of expressing extracellular depolymerases. MoPE was further studied for its ability to break down aliphatic polyesters PCL, PLA, PBS and PHB, but also the aliphatic-aromatic polyester PU. The degree of depolymerization was assessed through the decrease of the initial mass of the polymer, but also through the changes in average molecular weights ($\overline{M_n}$ $\overline{M_w}$) and molecular weight distribution (PDI) of the remaining polymers (Table 3). Interestingly, in all samples, the % $\overline{M_n}$ decrease was found higher than % $\overline{M_w}$ decrease resulting in slight broadening of the molecular weight distribution. Obviously, the shorter chains were the first to depolymerize due to their better diffusivity and ability to reach the active site of the enzyme. $\overline{M_n}$ is the average value representative of the total macromolecules number and it is much more sensitive to such cleavage reactions compared to weight-average molecular weight.

Turning to MoPE efficiency, the enzyme was found able to degrade all the target polymers to some extent, decreasing the mass of the polymer for four of them, meaning that it releases water-soluble products. Mass loss values along with changes in the molecular weight characteristics may reveal the prevailing scission mechanism, such as random or end scission pathways. PCL was the polymer that underwent the highest weight loss (33.4%), followed by PHB (8.9%), PBS (5.3%), PU (3.9%) while PLA did not show any mass decrease (Table 3). This ranking can be correlated to the polymers $T_g$ values (Table 2), since water diffusion rate and segmental mobility in the amorphous regions are decreased in high-$T_g$ matrices (Vey et al., 2012). In addition, the fact that PCL presented the highest mass loss while keeping high molecular weight ($\overline{M_n}$ decrease 10%) indicates end scission, i.e. mainly ester bonds at the end of the polymer chain were cleaved. On the other hand, for PLA where no gravimetrically observable weight loss was detected, random scission along the polymer backbone mainly occurred as evidenced by the 10.3% $\overline{M_n}$ decrease: the enzyme could cleave PLA chains in an endo-manner, but did not present any exo-activity, so as to release

**Table 3**
Percentage dry mass loss, $\overline{M_n}$, $\overline{M_n}$ percentage decrease, $\overline{M_w}$ and $\overline{M_w}$ percentage decrease after treating different polymers with MoPE.

| Polymer | Dry mass loss (%) | $\overline{M_n}$ (g/mol) | $\overline{M_n}$ decrease (%) | $\overline{M_w}$ (g/mol) | $\overline{M_w}$ decrease (%) | PDI |
|---|---|---|---|---|---|---|
| PCL | 33.4 ± 1.0 | 73700 ± 600 | 10.4 ± 3.0 | 107200 ± 500 | 1.7 ± 1.1 | 1.4 |
| MoPE-treated PCL | | 66000 ± 2700 | | 105400 ± 1200 | | 1.6 |
| PLA | 0.0 ± 0.0 | 100600 ± 300 | 10.2 ± 2.2 | 149900 ± 100 | 4.2 ± 3.1 | 1.5 |
| MoPE-treated PLA | | 90300 ± 2200 | | 143600 ± 4700 | | 1.6 |
| PBS | 5.3 ± 1.1 | 16100 ± 900 | 24.8 ± 5.9 | 27600 ± 1000 | 22.8 ± 4.4 | 1.7 |
| MoPE-treated PBS | | 12100 ± 200 | | 21300 ± 1300 | | 1.8 |
| PHB | 8.9 ± 2.9 | 177400 ± 8100 | 46.0 ± 6.9 | 219400 ± 10900 | 24.7 ± 4.3 | 1.2 |
| MoPE-treated PHB | | 95800 ± 5100 | | 165100 ± 9500 | | 1.7 |
| PU | 3.9 ± 1.9 | 66500 ± 500 | 4.1 ± 1.8 | 120800 ± 500 | 1.0 ± 0.8 | 1.8 |
| MoPE-treated PU | | 63800 ± 1200 | | 119600 ± 900 | | 1.9 |

water-soluble products and hence reduce the polymer mass (Fig. 8). On the other hand, MoPE showed a remarkable activity cleaving the chains of the remaining PHB, which was the polymer with the highest initial $\overline{M_n}$ (Table 2). In such case, a single random scission has a greater impact on molecular weight than end scission and controls thus molecular weight reduction (Shih, 1995). Accordingly, PHB suffered a loss in $\overline{M_n}$ of almost 50% with a low value of weight loss (8.9%). Similarly, the endo-activity of this enzyme on PBS is evident, with $\overline{M_n}$ decrease reaching 25% with a low value in mass loss (5.3%).

At this point, it is worth mentioning, that these results go beyond previous reports, showing that MoPE's ability to degrade PHB and PBS is absolutely promising. Lipases, cutinases and esterases are mentioned as potential PHB and PBS degrading enzymes, as they can extensively reduce the weight of PHB, PBS and their copolymers. A PHB depolymerase from *Alkaligenes faecalis*, which is an enzyme evolved for PHB degradation, when was tested on PHB polymer with similar properties to those used in this study, it reduced the weight of aged P(3-HB) and P(4-HB) films by 21% and 10%, respectively. Concerning PBS degradation, other lipases and esterases could reduce PBS weight in a similar extent, but after longer incubations compared to MoPE, proving that this enzyme has high potential in plastic degradation (Nikolaivits et al., 2021).

Finally, even though the weight loss and $\overline{M_n}$ decrease of MoPE-treated PU is low (3.9% and 4.1%, respectively), this is still an important finding, as this polymer is considered non or low-biodegradable in nature. For instance, LCC, which is one of the most efficient polyesterases for PU degradation (Nikolaivits et al., 2021), achieved 2.5–3.2% weight loss and around 18% $\overline{M_w}$ reduction (no $\overline{M_n}$ reduction) on two different polyester PU materials after 4 days at 70 °C (Schmidt et al., 2017).

## 4. Conclusions

The need for the discovery of novel and efficient plastic-degrading enzymes aiming to fight plastic pollution and develop an upcycling waste management process is imperative. Under this view, the potential of a psychrophilic esterase from *Moraxella* sp. for the degradation of non-biodegradable polymeric materials, such as PET and PU, as well as biodegradable synthetic polyesters, such as PCL, PHB, PBS and PLA, was investigated. The ability of the enzyme to hydrolyze the recalcitrant nature of plastics was investigated in a broad range of mass fraction crystallinity ranged from 11 up to 64%, indicating the ability of the enzyme to degrade highly crystalline materials. The utilization of the microbial lignocellulolytic degradation system seems to be the key for the efficient degradation of plastics, a fact that was highlighted by the synergy of the MoPE polyesterase with a ferulic acid esterase for the release of TPA from PET. The ability of MoPE to utilize highly crystalline synthetic polymers and its broad substrate range makes it an excellent template for enzyme engineering for the development of a robust plastic-degrading biocatalyst.

## Environmental implication

The uncontrollable disposal of plastic waste has raised global concern, as the consequences of plastics accumulation have now become apparent. Traditional recycling and incineration cannot effectively remedy the problem, but they are the only waste management alternatives instead of landfilling. However, the discovery of nature's mechanisms for breaking down plastic waste can result in a green, low-cost recycling technology. Specifically, novel enzymes with great potential in polymer degradation, can be a promising solution for the upcycling of urban plastic mix waste. An effective enzymatic arsenal can help repurposing and revalorizing plastics, whose impact has repercussions on ecosystem and human health.

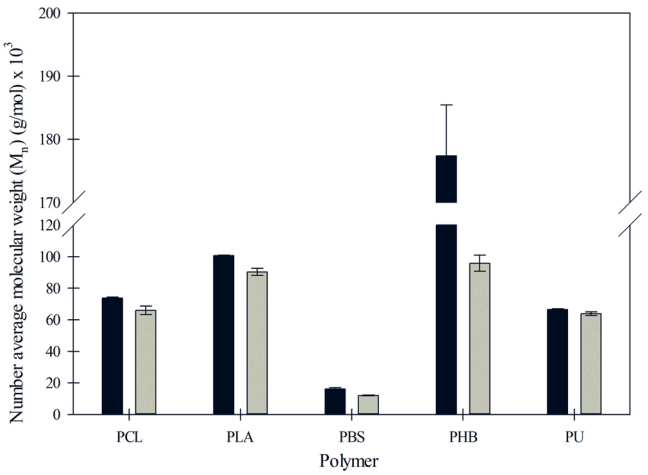


**Fig. 8.** Number average molecular weight of polymers before (black bars) and after (grey bars) treatment with MoPE at 30 °C after 3 days. $\overline{M_n}$ was determined by Gel Permeation Chromatography (GPC). Enzymatic reactions were performed in triplicates.

## Funding

This research was funded by European Union's Horizon 2020 research and innovation programme under grant agreement No 870292 (BioICEP Project) and by National Natural Science Foundation of China (Nos. 31961133016, 31961133015, and 31961133014).

## CRediT authorship contribution statement

**Efstratios Nikolaivits**: Conceptualization, Methodology, Validation, Investigation, Writing – original draft, Writing – review & editing, Visualization. **George Taxeidis**: Investigation, Writing – original draft, Writing – review & editing, Visualization. **Christina Gkountela**: Investigation, Writing – original draft, Visualization. **Stamatina Vouyiouka**: Methodology, Resources, Investigation, Writing – review & editing, Supervision. **Veselin Maslak**: Methodology, Resources. **Jasmina Nikodinovic-Runic**: Methodology, Resources, Investigation, Writing – review & editing. **Evangelos Topakas**: Conceptualization, Methodology, Validation, Resources, Writing – review & editing, Supervision, Funding acquisition. All authors read and approved the final manuscript.

## Declaration of Competing Interest

The authors declare that they have no known competing financial interests or personal relationships that could have appeared to influence the work reported in this paper.

## Acknowledgements

The authors would like to thank Dr Margaret Brennan Fournet from Technological University of the Shannon for providing the commercial polymeric materials.

## Appendix A. Supporting information

Supplementary data associated with this article can be found in the online version at doi:10.1016/j.jhazmat.2022.128900.

## References

Almagro Armenteros, J.J., Tsirigos, K.D., Sønderby, C.K., Petersen, T.N., Winther, O., Brunak, S., von Heijne, G., Nielsen, H., 2019. SignalP 5.0 improves signal peptide

predictions using deep neural networks. Nat. Biotechnol. 37, 420–423. https://doi.org/10.1038/s41587-019-0036-z.
Blank, L.M., Narancic, T., Mampel, J., Tiso, T., O'Connor, K., 2020. Biotechnological upcycling of plastic waste and other non-conventional feedstocks in a circular economy. Curr. Opin. Biotechnol. 62, 212–219. https://doi.org/10.1016/j.copbio.2019.11.011.
Blázquez-Sánchez, P., Engelberger, F., Cifuentes-Anticevic, J., Sonnendecker, C., Griñén, A., Reyes, J., Díez, B., Guixé, V., Richter, K.P., Zimmermann, W., Ramírez-Sarmiento, C.A., 2022. Antarctic polyester hydrolases degrade aliphatic and aromatic polyesters at moderate temperatures. Appl. Environ. Microbiol. 88. AEM.01842-21. https://doi.org/10.1128/AEM.01842-21.
Bollinger, A., Thies, S., Knieps-Grünhagen, E., Gertzen, C., Kobus, S., Höppner, A., Ferrer, M., Gohlke, H., Smits, S.H.J., Jaeger, K.-E., 2020. A novel polyester hydrolase from the marine bacterium *Pseudomonas aestusnigri* - Structural and functional insights. Front. Microbiol. 11, 114. https://doi.org/10.3389/fmicb.2020.00114.
Chamas, A., Moon, H., Zheng, J., Qiu, Y., Tabassum, T., Jang, J.H., Abu-Omar, M., Scott, S.L., Suh, S., 2020. Degradation rates of plastics in the environment, ACS Sustain. Chem. Eng. 8, 3494–3511. https://doi.org/10.1021/acssuschemeng.9b06635.
Chan, C.H., Kummerlöwe, C., Kammer, H.-W., 2004. Crystallization and melting behavior of Poly(3-hydroxybutyrate)-based blends. Macromol. Chem. Phys. 205, 664–675. https://doi.org/10.1002/macp.200300062.
Chen, C.-C., Han, X., Li, X., Jiang, P., Niu, D., Ma, L., Liu, W., Li, S., Qu, Y., Hu, H., Min, J., Yang, Y., Zhang, L., Zeng, W., Huang, J.-W., Dai, L., Guo, R.-T., 2021. General features to enhance enzymatic activity of poly(ethylene terephthalate) hydrolysis. Nat. Catal. 4, 425–430. https://doi.org/10.1038/s41929-021-00616-y.
Dimarogona, M., Nikolaivits, E., Kanelli, M., Christakopoulos, P., Sandgren, M., Topakas, E., 2015. Structural and functional studies of a *Fusarium oxysporum* cutinase with polyethylene terephthalate modification potential. Biochim. Biophys. Acta - Gen. Subj. 1850, 2308–2317. https://doi.org/10.1016/j.bbagen.2015.08.009.
Dimarogona, M., Topakas, E., Christakopoulos, P., Chrysina, E.D., 2020. The crystal structure of a *Fusarium oxysporum* feruloyl esterase that belongs to the tannase family, 1873-3468.13776 FEBS Lett.. https://doi.org/10.1002/1873-3468.13776.
Djapovic, M., Milivojevic, D., Ilic-Tomic, T., Lješević, M., Nikolaivits, E., Topakas, E., Maslak, V., Nikodinovic-Runic, J., 2021. Synthesis and characterization of polyethylene terephthalate (PET) precursors and potential degradation products: Toxicity study and application in discovery of novel PETases. Chemosphere 275, 130005. https://doi.org/10.1016/j.chemosphere.2021.130005.
Feller, G., Thiry, M., Gerday, C., 1990. Sequence of a lipase gene from the antarctic psychrotroph *Moraxella* TA144. Nucleic Acids Res. 18, 6431. https://doi.org/10.1093/nar/18.21.6431.
Filgueiras, V., Vouyiouka, S.N., Papaspyrides, C.D., Lima, E.L., Pinto, J.C., 2011. Solid-state polymerization of poly(ethylene terephthalate): the effect of water vapor in the carrier gas. Macromol. Mater. Eng. 296, 113–121. https://doi.org/10.1002/mame.201000201.
Furukawa, M., Kawakami, N., Oda, K., Miyamoto, K., 2018. Acceleration of enzymatic degradation of poly(ethylene terephthalate) by surface coating with anionic surfactants. ChemSusChem 11, 4018–4025. https://doi.org/10.1002/cssc.201802096.
Gasteiger, E., Hoogland, C., Gattiker, A., Duvaud, S., Wilkins, M.R., Appel, R.D., Bairoch, A., 2005. ProteiN Identification and Analysis Tools on The ExPASy Server. In: Walker, John M. (Ed.), Proteomics Protoc. Handb. Humana Press, Totowa, NJ, pp. 571–607. https://doi.org/10.1385/1-59259-890-0:571.
Georgousopoulou, I.-N., Vouyiouka, S., Dole, P., Papaspyrides, C.D., 2016. Thermo-mechanical degradation and stabilization of poly(butylene succinate). Polym. Degrad. Stab. 128, 182–192. https://doi.org/10.1016/j.polymdegradstab.2016.03.012.
Gkountela, C., Rigopoulou, M., Barampouti, E.M., Vouyiouka, S., 2021. Enzymatic prepolymerization combined with bulk post-polymerization towards the production of bio-based polyesters: the case of poly(butylene succinate). Eur. Polym. J. 143, 110197 https://doi.org/10.1016/j.eurpolymj.2020.110197.
Habib, S., Iruthayam, A., Abd Shukor, M.Y., Alias, S.A., Smykla, J., Yasid, N.A., 2020. Biodeterioration of untreated polypropylene microplastic particles by Antarctic bacteria. Polymers 12. https://doi.org/10.3390/polym12112616.
Jambeck, J.R., Geyer, R., Wilcox, C., Theodore, S.R., Perryman, M., Andrady, A., Narayan, R., Lavender Law, K., 2015. Plastic waste inputs from land into the ocean. Sci. (80-. ) 347, 768–771. https://doi.org/10.1126/science.1260352.
Kasprzyk, P., Sadowska, E., Datta, J., 2019. Investigation of thermoplastic polyurethanes synthesized via two different prepolymers. J. Polym. Environ. 27, 2588–2599. https://doi.org/10.1007/s10924-019-01543-7.
Kawai, F., Kawabata, T., Oda, M., 2019. Current knowledge on enzymatic PET degradation and its possible application to waste stream management and other fields. Appl. Microbiol. Biotechnol. 103, 4253–4268. https://doi.org/10.1007/s00253-019-09717-y.
Knott, B.C., Erickson, E., Allen, M.D., Gado, J.E., Graham, R., Kearns, F.L., Pardo, I., Topuzlu, E., Anderson, J.J., Austin, H.P., Dominick, G., Johnson, C.W., Rorrer, N.A., Szostkiewicz, C.J., Copié, V., Payne, C.M., Woodcock, H.L., Donohoe, B.S., Beckham, G.T., McGeehan, J.E., 2020. Characterization and engineering of a two-enzyme system for plastics depolymerization, 25476 LP – 25485 Proc. Natl. Acad. Sci. 117. https://doi.org/10.1073/pnas.2006753117.
Kumar, S., Stecher, G., Tamura, K., 2016. MEGA7: molecular evolutionary genetics analysis version 7.0 for bigger datasets. Mol. Biol. Evol. 33, 1870–1874. https://doi.org/10.1093/molbev/msw054.
Mohanan, N., Montazer, Z., Sharma, P.K., Levin, D.B., 2020. Microbial and enzymatic degradation of synthetic plastics (https://www.frontiersin.org/article/). Front. Microbiol 11. https://doi.org/10.3389/fmicb.2020.580709.
Moukouli, M., Topakas, E., Christakopoulos, P., 2008. Cloning, characterization and functional expression of an alkalitolerant type C feruloyl esterase from Fusarium oxysporum. Appl. Microbiol. Biotechnol. 79, 245–254. https://doi.org/10.1007/s00253-008-1432-3.
Mousavioun, P., Doherty, W.O.S., George, G., 2010. Thermal stability and miscibility of poly(hydroxybutyrate) and soda lignin blends. Ind. Crops Prod. 32, 656–661. https://doi.org/10.1016/j.indcrop.2010.08.001.
Napper, I.E., Davies, B.F.R., Clifford, H., Elvin, S., Koldewey, H.J., Mayewski, P.A., Miner, K.R., Potocki, M., Elmore, A.C., Gajurel, A.P., Thompson, R.C., 2020. Reaching new heights in plastic pollution—Preliminary findings of microplastics on Mount Everest. One Earth 3, 621–630. https://doi.org/10.1016/j.oneear.2020.10.020.
Narancic, T., O'Connor, K.E., 2019. Plastic waste as a global challenge: are biodegradable plastics the answer to the plastic waste problem? Microbiology 165, 129–137. https://doi.org/10.1099/mic.0.000749.
Nikolaivits, E., Kokkinou, A., Karpusas, M., Topakas, E., 2016. Microbial host selection and periplasmic folding in *Escherichia coli* affect the biochemical characteristics of a cutinase from *Fusarium oxysporum*. Protein Expr. Purif. 127, 1–7. https://doi.org/10.1016/j.pep.2016.06.002.
Nikolaivits, E., Dimarogona, M., Fokialakis, N., Topakas, E., 2017. Marine-derived biocatalysts: importance, accessing and application in aromatic pollutant bioremediation. Front. Microbiol 8, 265 http://journal.frontiersin.org/article/10.3389/fmicb.2017.00265/full (accessed February 8, 2017).
Nikolaivits, E., Kanelli, M., Dimarogona, M., Topakas, E., 2018. A middle-aged enzyme still in its prime: recent advances in the field of cutinases. Catalysts 8, 612. https://doi.org/10.3390/CATAL8120612.
Nikolaivits, E., Pantelic, B., Azeem, M., Taxeidis, G., Babu, R., Topakas, E., Brennan Fournet, M., Nikodinovic-Runic, J., 2021. Progressing plastics circularity: a review of mechano-biocatalytic approaches for waste plastic (re)valorization. Front. Bioeng. Biotechnol. 9, 535 https://www.frontiersin.org/article/10.3389/fbioe.2021.696040.
Patrício, T., Bártolo, P., 2013. Thermal stability of PCL/PLA blends produced by physical blending process. Procedia Eng. 59, 292–297. https://doi.org/10.1016/j.proeng.2013.05.124.
Peeken, I., Primpke, S., Beyer, B., Gütermann, J., Katlein, C., Krumpen, T., Bergmann, M., Hehemann, L., Gerdts, G., 2018. Arctic sea ice is an important temporal sink and means of transport for microplastic. Nat. Commun. 9, 1505. https://doi.org/10.1038/s41467-018-03825-5.
Pettersen, E.F., Goddard, T.D., Huang, C.C., Couch, G.S., Greenblatt, D.M., Meng, E.C., Ferrin, T.E., 2004. UCSF Chimera - A visualization system for exploratory research and analysis. J. Comput. Chem. 25, 1605–1612. https://doi.org/10.1002/jcc.20084.
Porfyris, A., Vasilakos, S., Zotiadis, C., Papaspyrides, C., Moser, K., Van der Schueren, L., Buyle, G., Pavlidou, S., Vouyiouka, S., 2018. Accelerated ageing and hydrolytic stabilization of poly(lactic acid) (PLA) under humidity and temperature conditioning. Polym. Test. 68, 315–332. https://doi.org/10.1016/j.polymertesting.2018.04.018.
Robert, X., Gouet, P., 2014. Deciphering key features in protein structures with the new ENDscript server. Nucleic Acids Res. 42, W320. https://doi.org/10.1093/nar/gku316.
Sagong, H.-Y., Son, H.F., Seo, H., Hong, H., Lee, D., Kim, K.-J., 2021. Implications for the PET decomposition mechanism through similarity and dissimilarity between PETases from *Rhizobacter gummiphilus* and *Ideonella sakaiensis*. J. Hazard. Mater. 416, 126075 https://doi.org/10.1016/j.jhazmat.2021.126075.
Schmidt, J., Wei, R., Oeser, T., Dedavid e Silva, L., Breite, D., Schulze, A., Zimmermann, W., 2017. Degradation of polyester polyurethane by bacterial polyester hydrolases. Polymers 9, 65. https://doi.org/10.3390/polym9020065.
Shih, C., 1995. Chain-end scission in acid catalyzed hydrolysis of poly (d,l-lactide) in solution. J. Control. Release 34, 9–15. https://doi.org/10.1016/0168-3659(94)00100-9.
Singh, A., Rorrer, N.A., Nicholson, S.R., Erickson, E., DesVeaux, J.S., Avelino, A.F.T., Lamers, P., Bhatt, A., Zhang, Y., Avery, G., Tao, L., Pickford, A.R., Carpenter, A.C., McGeehan, J.E., Beckham, G.T., 2021. Techno-economic, life-cycle, and socioeconomic impact analysis of enzymatic recycling of poly(ethylene terephthalate). Joule. https://doi.org/10.1016/j.joule.2021.06.015.
Thiyagarajan, S., Vogelzang, W., Knoop, R.J.I., Frissen, A.E., van Haveren, J., van Es, D. S., 2014. Biobased furandicarboxylic acids (FDCAs): effects of isomeric substitution on polyester synthesis and properties. Green. Chem. 16, 1957–1966. https://doi.org/10.1039/C3GC42184H.
Thomsen, T.B., Hunt, C.J., Meyer, A.S., 2022. Influence of substrate crystallinity and glass transition temperature on enzymatic degradation of polyethylene terephthalate (PET). N. Biotechnol. 69, 28–35. https://doi.org/10.1016/j.nbt.2022.02.006.
Tournier, V., Topham, C.M., Gilles, A., David, B., Folgoas, C., Moya-Leclair, E., Kamionka, E., Desrousseaux, M.-L., Texier, H., Gavalda, S., Cot, M., Guémard, E., Dalibey, M., Nomme, J., Cioci, G., Barbe, S., Chateau, M., André, I., Duquesne, S., Marty, A., 2020. An engineered PET depolymerase to break down and recycle plastic bottles. Nature 580, 216–219. https://doi.org/10.1038/s41586-020-2149-4.
Urbanek, A.K., Rymowicz, W., Mirończuk, A.M., 2018. Degradation of plastics and plastic-degrading bacteria in cold marine habitats. Appl. Microbiol. Biotechnol. 102, 7669–7678. https://doi.org/10.1007/s00253-018-9195-y.
Urbanek, A.K., Mirończuk, A.M., García-Martín, A., Saborido, A., de la Mata, I., Arroyo, M., 2020. Biochemical properties and biotechnological applications of microbial enzymes involved in the degradation of polyester-type plastics. Biochim. Biophys. Acta - Proteins Proteom. 1868, 140315 https://doi.org/10.1016/j.bbapap.2019.140315.

Urbanek, A.K., Strzelecki, M.C., Mirończuk, A.M., 2021. The potential of cold-adapted microorganisms for biodegradation of bioplastics. Waste Manag. 119, 72–81. https://doi.org/10.1016/j.wasman.2020.09.031.

Vey, E., Rodger, C., Meehan, L., Booth, J., Claybourn, M., Miller, A.F., Saiani, A., 2012. The impact of chemical composition on the degradation kinetics of poly(lactic-co-glycolic) acid copolymers cast films in phosphate buffer solution. Polym. Degrad. Stab. 97, 358–365. https://doi.org/10.1016/j.polymdegradstab.2011.12.010.

Vogel, C., Siesler, H.W., 2008. Thermal degradation of poly(ε-caprolactone), poly(L-lactic acid) and their blends with poly(3-hydroxy-butyrate) studied by TGA/FT-IR spectroscopy. Macromol. Symp. 265, 183–194. https://doi.org/10.1002/masy.200850520.

Wang, X., Zhou, J., Li, L., 2007. Multiple melting behavior of poly(butylene succinate). Eur. Polym. J. 43, 3163–3170. https://doi.org/10.1016/j.eurpolymj.2007.05.013.

Wu, K., Li, J., Chen, X., Yao, J., Shao, Z., 2020. Synthesis of novel multi-hydroxyl N-halamine precursors based on barbituric acid and their applications in antibacterial poly(ethylene terephthalate) (PET) materials. J. Mater. Chem. B. 8, 8695–8701. https://doi.org/10.1039/D0TB01497D.

Xiang, S., Feng, L., Bian, X., Li, G., Chen, X., 2020. Evaluation of PLA content in PLA/PBAT blends using TGA. Polym. Test. 81, 106211 https://doi.org/10.1016/j.polymertesting.2019.106211.

Yoshida, S., Hiraga, K., Takehana, T., Taniguchi, I., Yamaji, H., Maeda, Y., Toyohara, K., Miyamoto, K., Kimura, Y., Oda, K., 2016. A bacterium that degrades and assimilates poly(ethylene terephthalate). Science 351, 1196–1199. https://doi.org/10.1126/science.aad6359.